

Simulation Studies of Proton Transfer in N_2H_7^+ Cluster by Classical ab Initio Monte Carlo and Quantum Wave Packet Dynamics

Toshio Asada,* Haruya Haraguchi, and Kazuo Kitaura

Integrated Arts and Sciences, Osaka Prefecture University, 599-8531, Sakai-City, Japan

Received: December 15, 2000; In Final Form: May 22, 2001

The quantum effects on the proton-transfer reaction in the N_2H_7^+ cluster has been studied using the classical ab initio Monte Carlo method and a one-dimensional model for the quantum wave packet dynamics on the ab initio MP2/6-31+G* potential energy surface. The optimized stable structure has C_{3v} symmetry, in which the proton is bound to one NH_3 molecule in such a way that the proton feels bistable potential. In contrast, we found that the proton was located at the center of two NH_3 molecules with D_{3d} symmetry due to the quantum effects of the proton kinetics. The quantum simulations indicate that the reason the experimental spectra predict N_2H_7^+ to have a symmetric D_{3d} structure, contrary to the ab initio results, is that the quantum effects of the proton motion is completely neglected in the previous theoretical calculations. The vibrational frequency for the N–H stretching mode which corresponds to the proton transfer is estimated to be 706.7 cm^{-1} by including proton quantum effects in contrast with 2100.1 cm^{-1} obtained by the conventional ab initio MO method for the C_{3v} structure.

1. Introduction

The proton-transfer reaction plays an important role in many molecular systems such as cluster,^{1–9} liquid,¹⁰ crystal,¹¹ and so on, which are of particular interest with respect to the quantum phenomena. The proton-transfer processes are also related with the proton tunneling effects or proton disorder in hydrogen-bonded system observed in biomolecules. With these interests, hydrogen-bonded systems have been the subject of experimental and theoretical chemistry. In this respect, ammonia can be used as a prototype of the hydrogen-bound molecule.

Ammonia liquid has been studied using the Monte Carlo or molecular dynamics (MD) simulation,^{12,13} and many intermolecular potential functions have been proposed.^{6,14} However, the conventional classical simulations are not applicable to quantum problems even if we have good potential functions.

In this paper, we have investigated quantum effects on the bound proton in the N_2H_7^+ clusters. Ammoniated ammonium ions $\text{NH}_4^+(\text{NH}_3)_n$ are appropriate complexes as a prototype of weak hydrogen-bonded systems¹⁵ because the vibrational spectra have been measured experimentally¹⁶ and the model of the structure have been proposed for $n = 1–10$.¹⁷ In the theoretical point of view, Scheiner et al.⁵ reported that the calculation at the HF level with a minimal basis set gave the results that the hydrogen-bonded proton in N_2H_7^+ was midway between two nitrogen atoms. Increasing the basis set, on the other hand, the calculation gave a double-well potential with an energy barrier whose height decreased by the inclusion of polarizable electron correlation effect. Hirao et al.¹⁸ predicted an asymmetric C_{3v} structure using 3-21G basis set and Jaroszewski et al.⁶ showed that the potential depends largely on the N–N separation rather than on the proton position. Recently, Jursic¹⁹ reported the geometries and energies of the N_2H_7^+ clusters as well as H_5O_2^+ using the ab initio HF, MP2, G1, G2 methods with the 6-311G+(2d,2p) basis set, and the DFT methods with several

different exchange-correlation functionals. They mentioned that the low-level ab initio and DFT methods resulted in geometries for the complex composed of a proton and two ammonia molecules. However, the G2 calculation did not compute a symmetrical double ammonia complexed proton. Thus, the potential energy was considered to be extremely flat, therefore, it is very difficult to address the exact form. Interestingly, the experimental vibrational predissociation spectra by Price et al.¹⁶ suggest that the equilibrium structure is described by the formula $\text{H}_3\text{N}\cdots\text{H}^+\cdots\text{NH}_3$ rather than $\text{NH}_4^+\cdots\text{NH}_3$ despite this extremely flat potential energy surface.

The aim of the present work is to clarify quantum effects on the proton motion. We have used the quantum wave packet dynamics on the ab initio potential. To compare the structural results of the quantum simulation with that of the classical one, the classical MO-MC methods²⁰ have also been used.

2. Method

The ab initio MO calculations were carried out with the GAUSSIAN94 program.²¹ The geometry optimizations of the isomers, and the proton-transfer potential calculations for the wave packet dynamics were carried out using the MP2/6-31+G* level of theory. The zero-point energy (ZPE) were scaled by a recommended empirical factor of 0.91.²² In MC simulations, a huge number of energy calculations are required, then classical ab initio MC simulations were carried out at the HF/6-31G level of theory. To examine the quantum effects of the proton motion, the classical Monte Carlo calculations and the wave packet dynamics simulations were performed.

2.1. Classical MO-MC Simulation. We proposed a hybrid procedure of the ab initio molecular orbital (MO) and the classical Monte Carlo (MO-MC) samplings in the previous work. Details of the MO-MC algorithm were presented elsewhere.²⁰ For this MC samplings, both the rigid model and the nonrigid model are applied for trial moves. In the nonrigid model the unit for movement is an atom, whereas in the rigid model

* Author to whom correspondence should be addressed.

the unit is a molecule. Whether the rigid model or the nonrigid model is selected randomly at each movement. Because molecular units may be changed after the nonrigid model, the molecular units have to be redefined. To define the unit, a cluster analysis method with a threshold interatomic distance is used. The threshold used is 1.5 Å in this study. By this threshold, we confirmed that each molecular unit is reasonably defined at all steps in this study.

2.2. One-Dimensional Model for the Proton-Transfer Wave Packet Dynamics. The simplest model for the quantum wave packet dynamics for the proton-transfer reaction is a one-dimensional model on a potential energy surface along the intrinsic reaction coordinate (IRC). The one-dimensional discrete time-dependent Schrödinger equation is

$$i\hbar \frac{d\phi_n(t)}{dt} = \mathbf{H}\phi_n(t) \quad (1)$$

where $\phi_n(t)$ is the wave function at time t . If we rewrite $\phi_n(t)$ as $|\phi;t\rangle$, eq 1 is solved as

$$|\phi;t + \Delta t\rangle = \exp\left(\frac{-i\mathbf{H}}{\hbar}\Delta t\right)|\phi;t\rangle \quad (2)$$

Using the Taylor expansion, eq 2 can be written as

$$|\phi;t + \Delta t\rangle = \left[I - i\frac{\mathbf{H}}{\hbar}\Delta t + \frac{1}{2}\left(-i\frac{\mathbf{H}}{\hbar}\right)^2\Delta t^2 + \dots \right]|\phi;t\rangle \quad (3)$$

In our wave packet dynamics, the time development of the initial wave function was followed up the second order of Δt in eq 3.

The Hamiltonian \mathbf{H} can be divided into two parts;

$$\mathbf{H} = \mathbf{H}_0 + \mathbf{V} \quad (4)$$

Here, the $n \times n$ discrete representation of Hamiltonian matrix for the free particle \mathbf{H}_0 becomes

$$\mathbf{H}_0 = \frac{-\hbar^2}{2m(\Delta x)^2} \begin{pmatrix} -2 & 1 & & \mathbf{0} \\ 1 & \ddots & \ddots & \\ & \ddots & \ddots & 1 \\ \mathbf{0} & & & 1 & -2 \end{pmatrix} \quad (5)$$

where, Δx is the interval between neighboring positions x_i and x_{i+1} and m is the reduced mass. $\Delta x = 0.005$ Å, $n = 205$, and $m = 0.886$ u are used in this study.

The potential energy matrix \mathbf{V} can be expressed as

$$\mathbf{V} = \begin{pmatrix} V(x_1) & & \mathbf{0} \\ & \ddots & \\ \mathbf{0} & & V(x_N) \end{pmatrix} \quad (6)$$

In the limit $\Delta x \rightarrow 0$, these equations give the usual time-dependent wave equation;

$$i\hbar \frac{\partial}{\partial t}\phi(x,t) = \frac{-\hbar^2}{2m} \frac{\partial^2}{\partial x^2}\phi(x,t) + V(x)\phi(x,t) \quad (7)$$

The proton-transfer potential energy curve mainly depends on the intermolecular distance r_{NN} and the proton position x shown in Figure 1. In our IRC calculations, all structural parameters are optimized with respect to x . Usually, these are bistable

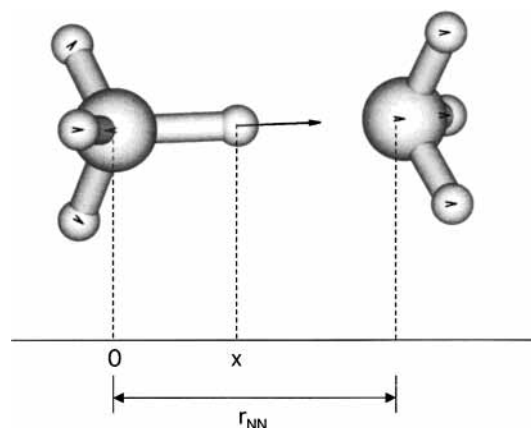


Figure 1. Model system and definition of the proton-transfer coordinate with the normal mode vector corresponding to the N–H stretching vibrational mode for the proton transfer.

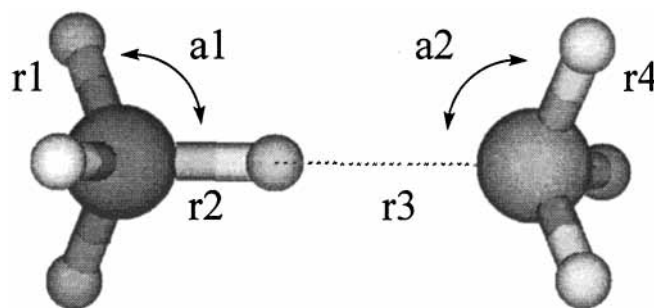
potentials as pointed out by Jaroszewski et al.⁶ Since the potential curve is calculated around the energy minimum to be valid in the range $0.80 < x < 1.82$ Å, the potential energy is modeled to be infinity at outside of this range.

3. Results and Discussion

3.1. Optimized Structure. The optimized stable and transition state structures of the N_2H_7^+ cluster were calculated using the ab initio HF, MP2, QCISD, and G2MP2 calculations with various basis sets. Table 1 summarized the structural parameters obtained by these calculations with the normal mode vibrational frequencies, the zero-point energy for the N–H stretching mode which corresponds to the proton transfer and the relative energy of the transition state based on each stable structure. At the G2MP2 level, only the optimized structure was obtained. The optimized stable structure was a linearly arranged $\text{NH}_4^+\cdots\text{NH}_3$ form with C_{3v} symmetry with a small barrier for the proton transfer already pointed out by Hirao et al.¹⁸ The N–H bond lengths, r_1 , r_2 , and r_4 , became longer by inclusion of the electron correlation effects resulting that the bound proton slightly moved to the center of the N–N bond. However, the hydrogen atom between the monomers is located at one side. The angles α_1 and α_2 did not significantly depend on the computational level in our calculations except for HF/6-31G result. Our optimized geometrical structures were in good agreement with the other theoretical results. On the other hand, the transition state structure had the linear arrangement proton bound $\text{NH}_3\cdots\text{H}^+\cdots\text{NH}_3$ form with D_{3d} symmetry. In a recent paper, Park²³ mentioned that the proton transfer did not take place in the N_2H_7^+ cluster.

It is clear that the activation energy ΔE for the proton transfer process is largely dependent on the computational level as shown in Table 1, which is decreased by the polarizable electron correlation calculations. Accidentally, HF/6-31G result indicates the smallest activation energy in our HF calculations. We should notice that the ZPE are higher than the activation energy for the HF/6-31G, MP2/6-31+G*, MP2/6-311++G**, and QCISD/6-311++G** calculations. These results suggest that the quantum effects on the proton transfer are quit important for this cluster.

3.2. Classical Monte Carlo Results. The MP2/6-31++G** level is almost 200 times time-consuming for single-point energy evaluations relative to the HF/6-31G level. To save the computational time for the ensemble averages, the HF/6-31G level of theory is applied on the following classical Monte Carlo simulations.

TABLE 1: The Structural Parameters with the Normal Mode Vibrational Frequencies for the N_2H_7^+ Cluster^a

	r_1 (Å)	r_2 (Å)	r_3 (Å)	r_4 (Å)	a_1 (deg)	a_2 (deg)	E (au)	freq (cm ⁻¹)	ZPE (kcal/mol)	ΔE (kcal/mol)
Stable Structure										
HF/6-31G	1.008	1.080	1.666	1.004	109.7	109.5	-112.72769	2189.1	3.13	
HF/6-31G*	1.010	1.060	1.755	1.006	110.1	112.6	-112.75700	2540.5	3.63	
HF/6-31+G*	1.010	1.054	1.792	1.006	110.0	112.7	-112.75894	2620.5	3.75	
HF/6-311++G**	1.009	1.057	1.766	1.005	110.0	112.6	-112.81044	2544.4	3.64	
MP2/6-31+G*	1.025	1.098	1.675	1.022	110.3	112.9	-113.10849	2100.1	3.00	
MP2/6-311++G**	1.021	1.120	1.574	1.019	110.6	113.1	-113.21511	1769.5	2.53	
QCISD/6-311++G**	1.022	1.101	1.624	1.020	110.5	113.3	-113.24409	1996.0	2.85	
G2MP2	1.025	1.115	1.616	1.021	110.5	112.8	-113.27456			
Transition State Structure										
HF/6-31G	1.006	1.295	1.295	1.006	110.0	110.0	-112.72423			2.17
HF/6-31G*	1.008	1.298	1.298	1.008	111.5	111.5	-112.75031			4.20
HF/6-31+G*	1.008	1.297	1.297	1.008	111.6	111.6	-112.75130			4.79
HF/6-311++G**	1.007	1.295	1.295	1.007	111.6	111.6	-112.80443			3.77
MP2/6-31+G*	1.024	1.308	1.308	1.024	111.8	111.8	-113.10575			1.72
MP2/6-311++G**	1.020	1.299	1.299	1.020	111.9	111.9	-113.21398			0.71
QCISD/6-311++G**	1.020	1.299	1.299	1.020	112.0	112.0	-113.24207			1.27

^a E is the energy. freq and ZPE mean the normal mode frequency and the zero-point energy for the N-H stretching mode for the proton transfer, respectively. ΔE is the relative energy based on each optimized structure.

To achieve the thermodynamic equilibrium condition, the first 50 000 moves are disregarded and the following 100 000 moves are used in this study. The radial distribution functions for N-H distances r_{NH} and N-N distances r_{NN} at $T = 100$ K are shown in Figures 2a and 2b, respectively. The distribution functions r_{NH} can be roughly classified into two groups. One is for the distance between the nitrogen atom and three connected hydrogen atoms directed to the outer side of cluster ranging from 0.95 to 1.05 Å, and the other is for the center hydrogen atom bridging two nitrogen atoms ranging from 1.00 to 1.15 Å. The peaks in the distribution function are close to the N-H distance of the optimized geometries. The peak positions for the center hydrogen atom is longer than that for the outside hydrogen atoms. The fluctuations are 0.1 and 0.15 Å for the terminal and bridge hydrogen, respectively. However, the proton transfer did not take place and the proton remains trapped in the reactant well during our simulation runs at $T = 100$ K. The peak of N-N radial distribution function is located at 2.74 Å, which is almost the same as the optimized structures, with rather large fluctuation from 2.6 to 2.9 Å. Thus, the equilibrium geometries can be concluded as the $\text{NH}_4^+ \cdots \text{NH}_3$ form from the classical simulations.

The classical simulations for this kind of system has already reported by Li et al.²⁴ In their recent investigation, the combined AM1/TIP3P molecular dynamics (MD) simulation at $T = 25$ °C was carried out for the proton-bound ammonia dimer in aqueous solution for the N_2H_7^+ model. In the same work, the distance between nitrogen atoms has been fixed at 2.62 Å, which is closer than the equilibrium position of 2.75 Å as shown in Table 1, so that proton-transfer events occur every 10–20 ps in average. These models are regarded as not realistic, because the N-N distance for the proton-transfer transition state is about

2.6 Å. Their model is too favorable to take the transition structure. In addition, the quantum effect for the proton kinetics are completely ignored. In our simulations at $T = 25$ °C, the proton transfer events was rarely observed although the fluctuation of intermolecular distance between NH_4^+ and the NH_3 molecule became significant.

3.3. Wave Packet Dynamics. The eigen vector for the normal mode associated with the proton-transfer reaction and the definition of the proton-transfer coordinate x are shown in Figure 1. Since there exists a large amplitude N-H stretching motion and very small motions of other atoms, we have applied a simple one-dimensional model for the proton-transfer process. In the following analysis we have used the one-dimensional potential curve calculated by ab initio MO method using the MP2/6-31+G* level of theory along with the intrinsic reaction coordinate (IRC). In the calculations, the structure optimization was carried out at each N-H distance x with the discrete step-size $\Delta x = 0.005$ Å.

The Hamiltonian matrix given in eq 4 was diagonalized to obtain the eigen states and the corresponding eigen values for the proton motion. Figure 3 illustrates the probability of appearance, which are square of eigenfunctions, and its eigen values together with the IRC potential curve. The IRC potential curve has bistable shape with a transition state. As all structural parameters are optimized at each N-H distance, the potential minimum and the transition state structure correspond to C_{3v} and D_{3d} symmetry, respectively.

The calculated eigen states confirm the importance of the quantum effect of the proton motion. Interestingly, the ground state, which has the energy of 1.79 kcal/mol, is not located at the optimized structure. However, there are broad peaks for the probability of appearance for the ground-state proton wave

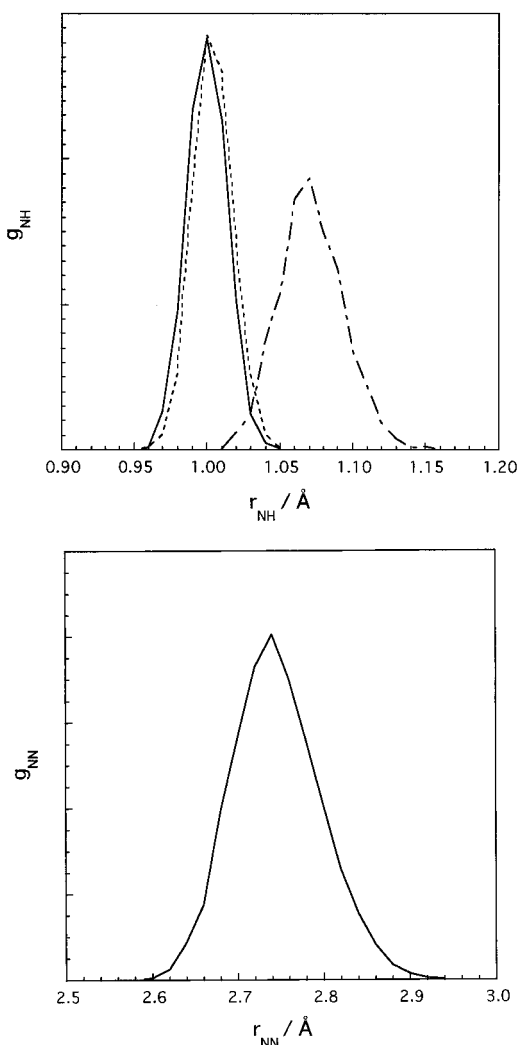


Figure 2. The radial distribution functions of the classical N_2H_7^+ cluster. Results are shown for simulations at 100 K where the protons were treated classically. (a) The N–H distance distributions. The r_1 distribution denoted by the solid line, the r_2 by the dashed line, and the r_3 by the dotted broken line (See Table 1). The r_2 distribution peak at about 1.07 Å corresponds to the optimized structure. (b) The N–N distribution which shows relatively large fluctuation about the optimized N–N distance.

function, and its maximum appears at the transition state structure at about 1.3 Å. These results lead to the conclusion that the ground-state structure is not the optimized structure but the transition state obtained from the ab initio MO calculation without quantum effects of proton. In the other words, the reason the experimental spectra by Price et al. predict N_2H_7^+ to have a symmetric D_{3d} structure, contrary to the ab initio results, is that the quantum effects of the proton motion is completely neglected in the previous theoretical calculations.

The first excitation state lies at the energy of 3.81 kcal/mol and shows a double peak centering around 1.10 and 1.51 Å corresponding to optimized structures. The stable structure obtained by ab initio MO calculations is expected to be the first excitation state considering the quantum effect of motion. In the first excitation state, the probability of appearance at the transition state structure becomes zero to give the orthogonality relation between two eigen states. The second excitation state lies at 8.09 kcal/mol which have three peaks at 1.02, 1.30, and 1.58 Å. Figure 3 shows the proton motion in this IRC potential curve looks like the trapped free particle motion in the harmonic potential well. The important point to note is that the transition

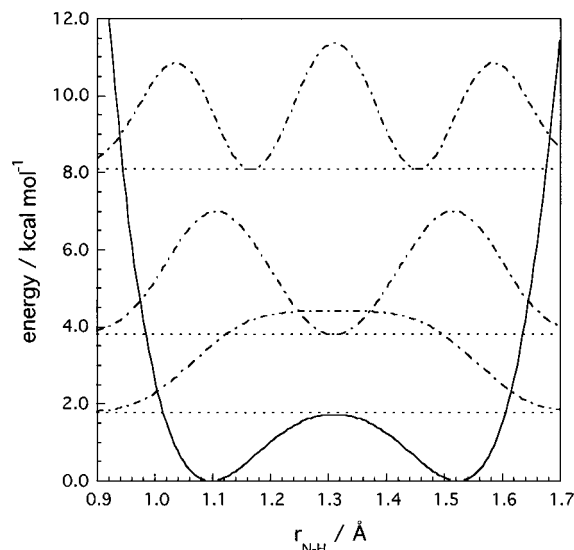


Figure 3. The IRC potential energy curve obtained by the MP2/6-311++G** level of theory (solid line), the probability of appearance for the bound proton (dotted broken line), which are square of the eigenfunctions, and the corresponding eigen values (dashed line). The IRC potential has bistable shape with a transition state which is just lower than the ground-state energy of the bound proton.

state structure has the relative energy of 1.72 kcal/mol from the stable structure, which is almost the same energy of the ground state for the quantum proton motion of 1.79 kcal/mol. In this case, the quantum effects is not negligible and the observable structure may be affected.

From the energy difference 2.02 kcal/mol between the ground state and the first excitation state, the frequency for the periodic motion of the proton-transfer reaction ω_{+-} can be determined. The frequency of de Broglie wave is related with the energy difference ΔE between the given two states:

$$h\omega_{+-} = \Delta E \quad (8)$$

where, h means Planck constant.

From the eigen state in Figure 3 the period of the proton transfer has been determined as $1/\omega_{+-} = 47.2$ fs at low energy. This results indicate that the proton transfer is a very quick event than the assumption of 10–20 ps estimated by Li et al.²⁴

The realistic behavior is more complicated than this simple model taking only two eigen states into account, because many eigen states would be affected to the quantum dynamics as the energy of the system increased. Then, we have carried out the quantum wave packet dynamics. The initial wave packet can be arbitrarily generated, however, the coherent state obtained by operating the translation operator on the ground-state wave function is used in our simulation. The five different initial states are considered. The expected values of the Hamiltonian for each initial wave packet are 1.79, 1.98, 2.74, 4.83, and 16.52 kcal/mol, respectively.

Figure 4 shows the time development of the wave packet for 100 ps with the energy of 2.74 kcal/mol. The distribution of protons has changed significantly for each time with the large principle vibration. The maximum position of the wave packet shifts to the potential well direction rather than the transition state at this energy for the most of the time.

The time development of the N–H distance for 300 ps is given in Figure 5 in which the distance is calculated between the N atom and the center of the mass for the bound proton wave packet. Figure 5 shows more clear periodic motions of the proton-transfer reaction. The center of mass for the ground-

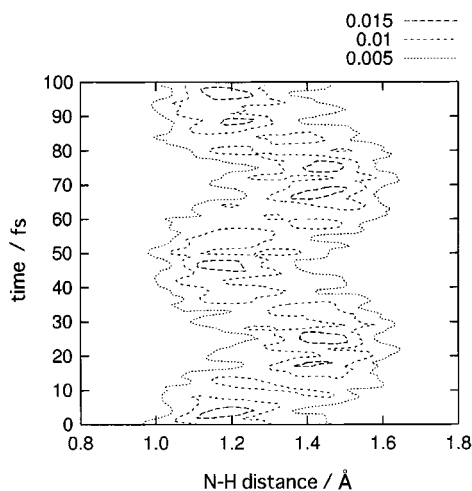


Figure 4. The time development of the wave packet with the energy of 2.74 kcal/mol. The period of the proton transfer is estimated to be about 45 fs.

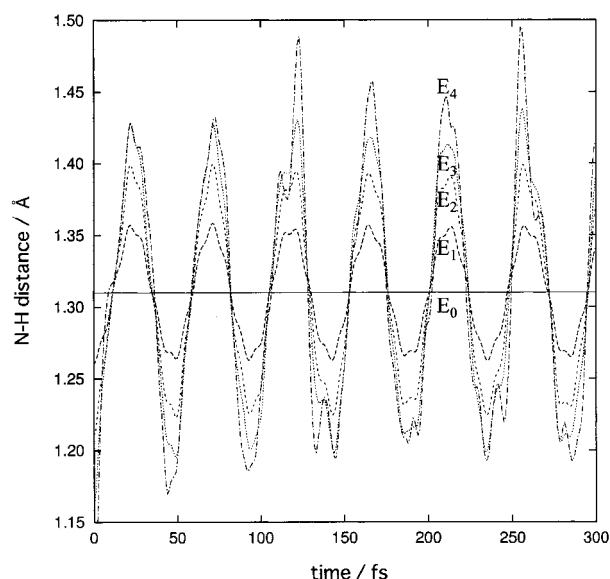


Figure 5. The time development of the N–H distance in which the distance is calculated between N atom and the center of the mass for the bound proton. The initial coherent wave packet has the different energy of the system. E_0 is 1.79 kcal/mol which means the ground state. E_1 , E_2 , E_3 , and E_4 are 1.98, 2.74, 4.83, and 16.52 kcal/mol, respectively.

state E_0 is located at 1.31 Å corresponding to the transition state at any time. Increasing the energy from E_1 to E_4 , increasing the amplitude of the proton motion. Though the amplitude of the proton motion largely depend on the energy considered, the period is almost the same for each energy. The period of the proton transfer is estimated to be about 45 fs which is coincident with the results 47.2 fs estimated above using only the ground state and the first excited state. We should notice that the amplitude of the proton motion can be easily changed even if only two lowest eigen states are taken into consideration. It is influenced by the mixing ratio of each state. It seems reasonable to suppose that Figure 5 includes two different components. One is the principal vibrational behavior corresponding to the proton transfer, which is mainly influenced by the lowest two eigen states, and the other is the small deviation affected by other relatively high energy eigen states. It can be concluded that the system energy changes the amplitude of the proton motion, however, it has rather small contribution on the period of the proton transfer in our study.

The vibrational frequency for the proton-transfer N–H stretching is estimated to be 706.7 cm^{-1} applying $1/\omega_{+-} = 47.2$ fs in contrast with 2100.1 cm^{-1} obtained by ab initio MO calculation for the C_{3v} optimized structure.

4. Summary

The quantum effects of the proton-transfer reaction in the N_2H_7^+ cluster has been studied using the classical ab initio Monte Carlo and a one-dimensional model for the quantum wave packet dynamics on the ab initio MP2/6-31+G* potential energy surface. The optimized stable structure has C_{3v} symmetry, in which the proton is bound with one NH_3 molecule in such a way that the proton-transfer process feels bistable potential. In contrast, we found that the proton is located at the center of two NH_3 molecules with D_{3d} symmetry due to the quantum effects of the proton kinetics. The energy barrier for the proton-transfer process in N_2H_7^+ cluster is 1.72 kcal/mol, which is almost the same energy of the ground state for the quantum proton motion of 1.79 kcal/mol. In this case, the double well potential curve looks like the single harmonic potential well, therefore the quantum effects are not negligible and the observable structure may be affected. The reason the experimental spectra by Price et al. predict N_2H_7^+ to have a symmetric D_{3d} structure, contrary to the ab initio results, is that the quantum effects of the proton motion are completely neglected in the previous theoretical calculations. The results of the wave packet dynamics indicate that the system energy changes the amplitude of the proton motion, however, it has rather small contribution on the period of the proton transfer to be about 45 fs. The vibrational frequency for the N–H stretching mode which corresponds to the proton transfer is estimated to be 706.7 cm^{-1} in contrast with 2100.1 cm^{-1} obtained by the ab initio MO method for the C_{3v} structure.

Acknowledgment. This work was supported by a Grant-in-Aid for advanced scientific research from Osaka Prefecture University and was also partially supported by the Ministry of Education, Science, Sports and Culture, Grant-in-Aid for Encouragement of Young Scientists, 14740325, 2000. The part of the calculation was carried out at the computer center in the institute of the molecular science in Okazaki.

References and Notes

- (1) Snyder, E. M.; Castleman, A. W., Jr. *J. Chem. Phys.* **1997**, *107*, 744.
- (2) Angle, L.; Stace, A. J. *J. Chem. Phys.* **1998**, *109*, 1713.
- (3) Ye, L.; Cheng, H.-P. *J. Chem. Phys.* **1998**, *108*, 2015.
- (4) Cheng, H.-P. *J. Chem. Phys.* **1996**, *105*, 6844.
- (5) Scheiner, S.; Harding, L. B. *J. Am. Chem. Soc.* **1981**, *103*, 2169.
- (6) Jaroszewski, L.; Lesyng, B.; McCammon, J. A. *J. Mol. Struct. (THEOCHEM)* **1993**, *283*, 57.
- (7) Cazar, R.; Jamka, A.; Tao, F.-M. *Chem. Phys. Lett.* **1998**, *287*, 549.
- (8) Stich, I.; Marx, D.; Parrinello, M.; Terakura, K. *J. Chem. Phys.* **1997**, *107*, 9482.
- (9) Cazar, R. A.; Jamka, A. J.; Tao, F.-M. *J. Phys. Chem.* **1998**, *102*, 5117.
- (10) Komatsuzaki, T.; Iwao, O. *Mol. Simul.* **1996**, *16*, 321–344.
- (11) Shimizu, A.; Tachikawa, H. *Chem. Phys. Lett.* **1999**, *314*, 516.
- (12) Honda, K.; Kitaura, K.; Nishimoto, K. *Bull. Chem. Soc. Jpn.* **1994**, *67*, 2679.
- (13) Diraison, M.; Martyna, G. J.; Tuckerman, M. E. *J. Chem. Phys.* **1999**, *111*, 1096.
- (14) Mauro, F.; Michael, H.; Ian, M. R.; Michael, K. L. *J. Chem. Phys.* **1990**, *93*, 5156.
- (15) Platts, J. A.; Laidig, K. E. *J. Phys. Chem.* **1995**, *99*, 6487.
- (16) Price, J. M.; Crofton, M. W.; Lee, Y. T. *J. Phys. Chem.* **1991**, *95*, 2182.
- (17) Ichihashi, M.; Yamabe, J.; Murai, K.; Nonose, S.; Hirao, K.; Kondow, T. *J. Phys. Chem.* **1996**, *100*, 10050.

- (18) Hirao, K.; Fujikawa, T.; Konishi, H.; Yamabe, S. *Chem. Phys. Lett.* **1984**, *104*, 184.
- (19) Jursic, B. S. *J. Mol. Struct. (THEOCHEM)* **1997**, *393*, 1.
- (20) Asada, T.; Iwata, S. *Chem. Phys. Lett.* **1996**, *260*, 1.
- (21) Frish, M. J.; Trucks, G. W.; Schlegel, H. B.; Gill, P. M. W.; Johnson, B. G.; Robb, M. A.; Cheeseman, J. R.; Keith, T. A.; Petersson, G. A.; Montgomery, J. A.; Raghavachari, K.; Al-Lahem, M. A.; Zakrzewski, V. G.; Ortiz, J. V.; Foresman, J. B.; Cioslowski, J.; Stefanov, B. B.; Nanayakkara, A.; Challacombe, M.; Peng, C. Y.; Ayala, P. Y.; Chen, W.; Wong, M. W.; Andres, J. L.; Replogle, E. S.; Gomperts, R.; Martin, R. L.; Fox, D. J.; Binkley, J. S.; Defrees, D. J.; Baker, J.; Stewart, J. P.; Head-Gordon, M.; Gonzales, C.; Pople, J. A. In *Gaussian*; Gaussian, Inc.: Pittsburgh, PA, 1995.
- (22) Pople, J. A.; Scott, A. P.; Wong, M. W.; Random, I. *Isr. J. Chem.* **1993**, *33*, 345.
- (23) Park, J. K. *Bull. Korean Chem. Soc.* **1999**, *20*, 1071.
- (24) Li, G.-S.; Martines Costa, M. T. C.; Millot, C.; Ruiz-Lopez, M. F. *Chem. Phys.* **1999**, *240*, 93.